Microchimica Acta (2019) 186: 407
https://doi.org/10.1007/s00604-019-3518-2

ORIGINAL PAPER

Preparation of a glassy carbon electrode modified with reduced graphene oxide and overoxidized electropolymerized polypyrrole, and its application to the determination of dopamine in the presence of ascorbic acid and uric acid

Xia Chen[1] · Dandan Li[1] · Weina Ma[1] · Tianfeng Yang[1] · Yanmin Zhang[1] · Dongdong Zhang[1]

Received: 7 January 2019 / Accepted: 19 May 2019 / Published online: 10 June 2019

Abstract
This paper presents a method for the preparation of a graphene-based hybrid composite film by electrodeposition of reduced graphene oxide and overoxidized electropolymerized polypyrrole onto a glassy carbon electrode (GCE) using cyclic voltammetry. The morphology of the hybrid composite film was characterized by scanning electron microscopy. The electrochemical activity of the modified GCE was studied by cyclic voltammetry using the negatively charged redox probe $Fe(CN)_6^{3-}$ and the positively charged redox probe $Ru(NH_3)_6^{3+}$. The modified GCE displays excellent electrocatalytic activity for dopamine (DA) and uric acid (UA), but electrostatically repulses ascorbate anion under physiological pH conditions. The voltammetric response to DA is linear in the 2.0 μM to 160 μM concentration range even in the presence of 1.0 mM ascorbic acid and 0.1 mM of UA. The detection limit is 0.5 μM. The amperometric response to DA (best measured at 0.22 V vs. Ag/AgCl) extends from 0.4 μM to 517 μM and has a 0.2 μM detection limit.

Keywords Graphene · Polypyrrole · Hybrid composite · Nanocomposite · Modified electrode · Neurotransmitter · Electrochemical sensor

Introduction

Dopamine (DA) is an important neurotransmitter in the mammalian central nervous system and associated with various kinds of diseases [1]. Hence, it is important to develop simple, rapid, selective and sensitive analytical methods for the detection of DA. Over the past years, great progress has been made in electrochemical DA biosensor [2, 3], however, many analytical challenges remain to be worked out, one of which is the interference of the coexistence of ascorbic acid (AA) and uric acid (UA) for the electrochemical determination of DA. The oxidation peak potentials of AA, DA and UA at bare electrode can't be distinguished clearly and the oxidation product will partly foul the electrode. Thus, the development of special materials employed to modify electrode to improve the sensitivity and selectivity for the determination of DA in the presence of interfering compounds is imperative. Electrodeposited reduced graphene oxide (RGO) combined with poly-L-lysine [4], zinc-nickel nanoparticles decorated multiwalled carbon nanotube [5], and cadmium selenide quantum dots coated with RGO [6] nanocomposites have been successfully applied to simultaneous voltammetric determination of AA, DA and UA. Furthermore, the AA concentration is much higher (100–1000 times) than that of DA in body fluids. Therefore, selective detection of DA and UA, and even their simultaneous detection in the presence of large amounts of AA are very crucial in diagnostic and pathological researches. Recently, Li et al. reported simultaneous determination of DA and UA in the presence of

Electronic supplementary material The online version of this article (https://doi.org/10.1007/s00604-019-3518-2) contains supplementary material, which is available to authorized users.

✉ Dongdong Zhang
ddzhang@xjtu.edu.cn

[1] School of Pharmacy, Xi'an Jiaotong University, Xi'an 710061, China

AA using gold electrode modified with carboxylated graphene and silver nanocube functionalized polydopamine nanospheres [7]. However, it is very necessary to further improve the analytical performance for the DA detection based on the development of novel electrode modification materials.

Polypyrrole (PPy), an important conductive polymer with conjugated structure, has been extensively applied in drug delivery [8], biosensor [9] and capacitor [10] since it was synthesized by electrochemical polymerization of pyrrole monomer by Diaz [11] due to its high conductivity, facile fabrication and good stability. In addition, PPy can be electrochemically oxidized to overoxidized polypyrrole (OPPy) incorporating a great deal of carbonyl groups [12] which endows OPPy with unique cation selectivity [13–15] and exclusion of anionic species [16]. Based on this, OPPy is expected to realize the selective detection of DA and to minimize the interference of AA. However, it should be noted that the overoxidization of PPy will disturb the conjugation and lead to the ionically conductive and has ion-selective properties but electronically nonconductive [12, 15] that goes against the electrochemical signal collection. Nanomaterials with high electronic conductivity and novel catalytic activity have been widely used as modifier to improve electrode conductivity and electrocatalytic activity in bioanalytical applications [17]. Graphene is a desirable candidate, was discovered by Geim and his coworkers in 2004 [18], which has been widely applied in electrochemical sensing and biosensing field [19, 20] owing to its huge surface area, high conductivity and superior biocompatibility etc.

Here, we combined the unique advantages of graphene with superior cation selective property of overoxidized polypyrrole by electropolymerization to construct a graphene-based hybrid nanocomposite film modified electrode. The combination of graphene with conducting polymers is beneficial, since graphene can immensely improve the electrical conductivity and mechanical strength of the resulting polymer-graphene hybrids, because of their unique properties and their geometry, which provides a three-dimensional nanostructure with a large electroactive area. The electrochemical reduction and deposition processes of GO, the electropolymerization process of pyrrole and the overoxidation process of polypyrrole were conducted by cyclic voltammetry. And the surface morphology of the modified electrodes was characterized by scanning electron microscopy. Furthermore, the electrochemical properties and the electrocatalytic activities towards AA, DA and UA of the modified electrodes were investigated. Finally, the electrochemically voltammetric and amperometric analysis methods for the selective and sensitive determination of DA in the presence of AA and UA under physiological pH conditions were presented.

Experimental

Materials and apparatus

Graphene oxide (GO) was purchased from Nanjing XFNANO Materials Tech Co., Ltd. (www.xfnano.com). Pyrrole, ascorbic acid (AA), dopamine (DA), uric acid (UA), Potassium ferricyanide and Hexaammineruthenium(III) chloride were purchased from Sigma-Aldrich (www.sigmaaldrich.com). All reagents were of analytical grade, and Millipore Milli-Q water (18.2 MΩ cm) was used throughout.

Scanning electron microscopic (SEM) image was obtained with Gemini SEM 500 (Zeiss, Germany). Electrochemical measurements were conducted by using a computer-controlled CHI760 electrochemical workstation (Shanghai CH Instruments, www.chinstruments.com) with a conventional three-electrode system consisted of platinum wire as an auxiliary electrode, a saturated Ag/AgCl electrode as a reference electrode and a bare or modified glassy carbon electrode (GCE, diameter 3.0 mm) as working electrode at room temperature. Electrolyte solution was 10 mM sodium phosphate buffer saline (PBS, pH 7.4) which was deoxygenated with highly purity nitrogen for 10 min before each measurement.

Preparation of modified electrodes

The fabrication procedure of OPPy/ERGO/GCE was illustrated in Scheme 1. Firstly, the bare GCE was polished to a mirror finish with 0.3 μm and 0.05 μm Al_2O_3 powder followed by ultrasonicating in ethanol and tri-distilled water for 5 min, respectively, and rinsing thoroughly with tri-distilled water. Then, electrochemically reduced graphene oxide film was fabricated on the clean bare GCE by cyclic voltammetry between 0.6 V and − 1.5 V for 8 cycles, in the N_2-saturated 10 mM PBS (pH 7.4) containing 0.4 mg mL^{-1} GO under a continuously magnetic stirring at scan rate of 25 mV s^{-1} (marked as ERGO/GCE). After then, the ERGO/GCE was subjected to cyclic voltammetric scanning between −0.2 V and 0.8 V for 8 cycles, in the 10 mM PBS (pH 7.4) containing 0.2 M pyrrole at 100 mV s^{-1} (marked as PPy/ERGO/GCE). Finally, PPy/ERGO/GCE was electrochemically overoxidized by cyclic voltammetry between 0 V and 1.0 V for 4 cycles, in the 0.1 M NaOH aqueous solution at scan rate of 100 mV s^{-1} (marked as OPPy/ERGO/GCE). For comparison, PPy/GCE and OPPy/GCE were also prepared respectively according to the same preparation methods above.

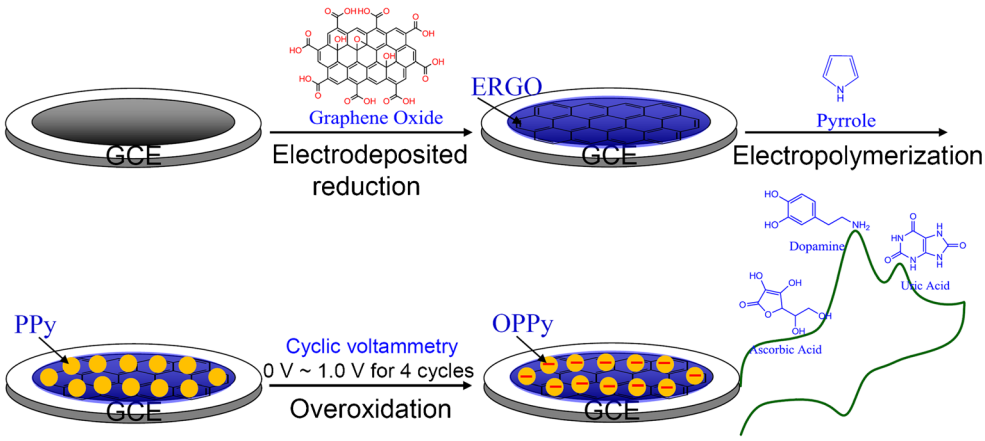

Scheme 1 Schematic diagram of the fabrication procedure of OPPy/ERGO/GCE.

Results and discussion

Electrochemical characterization of the glassy carbon electrode modified with overoxidized electropolymerized polypyrrole and electrochemically reduced graphene oxide (OPPy/ERGO/GCE)

Figure 1a shows the electrodeposition and reduction process of GO on a bare GCE by cyclic voltammetry with the potential window of +0.6 V to −1.5 V. An irreversible reduction peak can been obviously observed at the potential range of −1.0 V to −1.5 V which was attributed to the irreversible reduction process of the oxygen-containing groups of GO. Furthermore, the irreversible reduction peak currents persistently increasing with scanning cycles, suggesting that the ERGO deposited successfully on the GCE surface [21, 22]. Figure 1b shows the electropolymerization process of pyrrole monomer on the ERGO/GCE between −0.2 V and + 0.8 V. An oxidation peak occurs with a starting potential of about +0.5 V and the charging currents gradually increasing with the scanning cycles. This indicates that the electrochemical polymerization of pyrrole monomer on the ERGO/GCE has been achieved [23]. Figure 1c shows the overoxidization of the polypyrrole film in 0.1 M NaOH. The amplitude of the currents decrease with each successive voltage scan, suggesting that the film gradually loses its electrochemical conductivity [16]. This overoxidation procedure was repeated four scanning cycles while the currents were closed to a stable value to ensure complete coverage, which indicates that the overoxidized polypyrrole film has been obtained.

Morphologic characterization of modified GCE

Figure 2 displays the SEM images of the PPy/ERGO films before and after overoxidation treatment in 0.1 M NaOH aqueous solution. Figure 2a shows laminated structures of PPy/ERGO film on the GCE surface. And multiple small globes or spheres like structure of PPy are fully covering on the surface of PPy/ERGO film (Fig. 2b). This indicates that the three-dimensional polymeric structures can be electrochemically synthesized in situ on the electrode surface by a template method. The method involves precipitation polymerization in the presence of an effective graphene template which confines the growth of the PPy polymer to the graphene template-solution interface, resulting in the formation of a PPy polymeric replica [24]. After electrochemical overoxidation treatment, a rough, uniform and compact thin film is successfully achieved on the modified electrode surface (Fig. 2c), moreover, the large number of edges of paper-like sheets with wrinkled areas is observed (Fig. 2d). This typical wrinkling structure and homogeneously distributed hybrid film has unique electrochemical properties due to the formation of a large fraction of OPPy polymeric composite film with ERGO edge-plane defects, which can provide a higher surface activity than before treatment of the PPy/ERGO film [25].

Electrochemical activity of the glassy carbon electrode modified with overoxidized electropolymerized polypyrrole and electrochemically reduced graphene oxide (OPPy/ERGO/GCE)

The redox probes selected are important and representative electroactive compounds, with the similar size, fast electron transfer kinetics on carbon electrodes but with opposite charges. The electrochemical activities of bare GCE, ERGO/GCE, PPy/ERGO/GCE and OPPy/ERGO/GCE in the negatively charged probe $Fe(CN)_6^{3-}$ system and positively charged probe $Ru(NH_3)_6^{3+}$ system were investigated, respectively. In the case of $Fe(CN)_6^{3-}$ test system (Fig. 3a), it can be observed that a pair of reversible redox peaks at bare GCE (curve a) with the peak potential separation (ΔE_p) of 78 mV and the ratio of oxidation peak current to reduction peak current (i_{pa}/i_{pc}) is close to 1.0. While at the ERGO/GCE (curve b), the redox peak currents clearly increase to 1.9-times of that at bare GCE, and the value of ΔE_p slightly changes to 64 mV. This can be attributed to the fact that graphene has a large surface area due to its wrinkle-like structure [22] and excellent electronic conductivity [26]. For the PPy/ERGO/GCE (curve c), it can be seen that the background

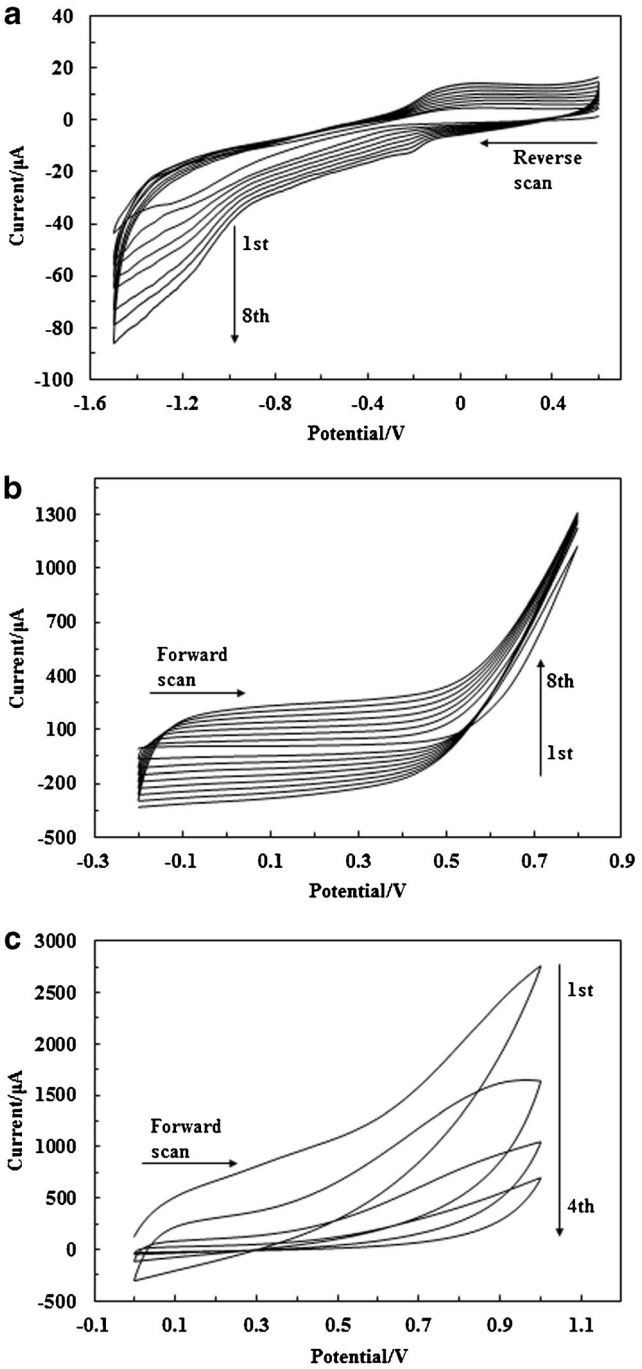

Fig. 1 **a** Cyclic voltammograms on bare GCE in N_2-saturated 10 mM PBS (pH 7.4) containing 0.4 mg mL^{-1} GO under a continuously magnetic stirring at scan rate of 25 mV s^{-1}. **b** Cyclic voltammograms on ERGO/GCE<?thyc= in 10 mM PBS (pH 7.4) containing 0.2 M pyrrole at 100 mV s^{-1}. **c** Cyclic voltammograms on PPy/ERGO/GCE in 0.1 M NaOH aqueous solution at 100 mV s^{-1}

charge currents dramatically increased, while the redox peak currents clearly decreased and the value of ΔE_p broadens to 146 mV. This is probably owing to PPy with high energy storage capacity and good electrical conductivity [27]. At the OPPy/ERGO/GCE (curve d), in contrast, the background charge currents decreased, but the redox peaks for hexacyanoferrate(III) probe is absent. This suggests that the negatively charged probe does not reach the electrode surface to take place in the electron transfer because the OPPy film (with its negative charge) causes electrostatic repulsion.

In the case of $Ru(NH_3)_6^{3+}$ system (Fig. 3b), it can be seen that there are a pair of redox peaks on the bare GCE (curve a), with the oxidation peak potential at −0.116 V, the reduction peak potential at −0.181 V, and the formal potential $E_{1/2}$ is −0.149 V. While at the ERGO/GCE (curve b), the redox peak currents clearly increased and the oxidation peak potential negatively shifts to −0.132 V, the reduction peak potential negatively shifts to −0.194 V, and the formal potential $E_{1/2}$ is −0.163 V. For the PPy/ERGO/GCE (curve c), it also can be seen that the background charge currents dramatically increased and the redox peaks even disappeared. While at the OPPy/ERGO/GCE (curve d), the background charge currents decreased, as well as the redox peaks of the $Ru(NH_3)_6^{3+}$ reappears at −0.253 V of oxidation peak potential, at −0.327 V of reduction peak potential, and the formal potential $E_{1/2}$ is −0.290 V. Furthermore, the oxidation peak current increase to 4.7-times and the reduction peak current clearly increase to 9.3-times of that at bare GCE, respectively. This result indicates that the positively charged probe Hexaammineruthenium(III) convenient to reach the electrode surface to take place in the electron transfer since the OPPy film (with its negative charge) causes electrostatic adsorption.

The results demonstrates that the OPPy/ERGO hybrid nanocomposite film with excellent ion-selective properties, which with negative charge hinders the anion and promotes the cation to reach the electrode surface to take place in the electron transfer. Additionally, comparison of the electrochemical activity between OPPy/ERGO/GCE and PPy/ERGO/GCE in the both $Fe(CN)_6^{3-}$ system and $Ru(NH_3)_6^{3+}$ system, suggesting that the overoxidation process has the crucial significance on the electrochemical activity of the PPy/ERGO hybrid nanocomposite.

Electrochemical catalysis of OPPy/ERGO/GCE towards AA, DA and UA

The electrochemical behaviors of AA, DA and UA on bare GCE, OPPy/GCE, ERGO/GCE and OPPy/ERGO/GCE were investigated by cyclic voltammetry. In Fig. 4a, compared with the bare GCE (curve a), the oxidation peak potential of AA positively shifts from +0.146 V to +0.185 V, and the oxidation peak current decreases from 14.1 μA to 7.5 μA at the OPPy/GCE. This mainly due to that the poor conductivity and anion exclusion of OPPy film (AA with negative charge under physiological pH conditions). For the ERGO/GCE (curve c), the oxidation peak potential of AA negatively shifts from +0.146 V to −0.001 V, and the oxidation peak current increases from 14.1 μA to 16.9 μA. While at the OPPy/ERGO/GCE (curve d), the oxidation peak of the AA is absent, suggesting that the OPPy/ERGO hybrid nanocomposite film can effectively hinders AA electron transfer.

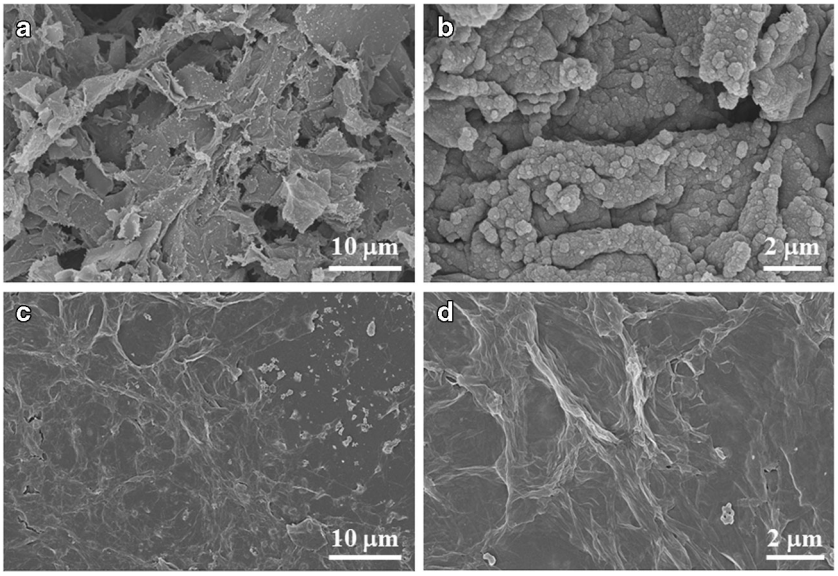

Fig. 2 Scanning electron microscopy images of PPy/ERGO/GCE (**a** and **b**) and OPPy/ERGO/GCE (**c** and **d**)

In Fig. 4b, it can be observed that the oxidation peak potential and reduction peak potential of DA at bare electrode appears at +0.181 V and + 0.139 V, and the ΔE_p is 39 mV and the $E_{1/2}$ is +0.159 V. Compared with the bare GCE, the ΔE_p is 35 mV and the $E_{1/2}$ is +0.157 V at the OPPy/GCE, the ΔE_p is 34 mV and the $E_{1/2}$ is +0.168 V at the ERGO/GCE, and the ΔE_p is 47 mV and the $E_{1/2}$ is +0.159 V at the OPPy/ERGO/GCE, respectively. Furthermore, the oxidation peak current at the OPPy/ERGO/GCE (27.4 μA) is 1.9, 9.8 and 11.9 times of that at the ERGO/GCE (14.3 μA), OPPy/GCE (2.8 μA) and bare GCE (2.3 μA), and the reduction peak current at the OPPy/ERGO/GCE (10.7 μA) is 2.2, 8.2 and 8.9 times of that at the ERGO/GCE (4.9 μA), OPPy/GCE (1.3 μA) and bare GCE (1.2 μA) respectively. This indicates that the OPPy/ERGO/GCE has excellent electrocatalytic activity towards DA due to that the OPPy/ERGO hybrid nanocomposite film can effectively accelerates DA electron transfer.

In Fig. 4c, the oxidation peak current of UA at the OPPy/ERGO/GCE (15.0 μA) is 4.8, 13.6 and 18.7 times of that at the ERGO/GCE (3.1 μA), OPPy/GCE (1.1 μA) and bare GCE (0.8 μA), respectively, indicating that OPPy/ERGO/GCE has electrochemical catalytic effect on the oxidation of UA. In order to further investigate the electrocatalysis and ion-selectivity of OPPy/ERGO, the coexistence system of AA, DA and UA was investigated by cyclic voltammetry. From Fig. 4d, it can be seen that the oxidation peaks of AA, DA and UA completely overlaped and shows a broad peak at +0.197 V for the bare GCE, at +0.189 V for the OPPy/GCE, respectively. While at the ERGO/GCE, the oxidation peaks of AA, DA and UA are separated well and appears at +0.009 V, +0.206 V and + 0.346 V. Interestingly, at the OPPy/ERGO/GCE, the behavior similar with that of the single component of AA system (Fig. 4a), the oxidation peak of AA is effectively absent. There are just two oxidation peaks at +0.205 V and + 0.371 V which corresponding to that the oxidation peak potentials of DA and UA. These results indicates that OPPy/ERGO/GCE with superior electrocatalysis and selectivity properties towards DA, which probably attributed to that the electrocatalytic activity of graphene and the cation

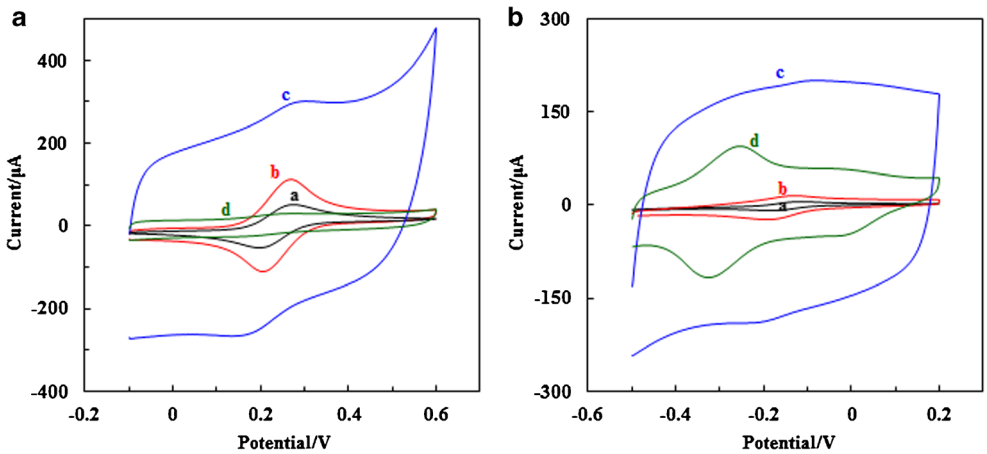

Fig. 3 Cyclic voltammograms in N_2-saturated 10 mM PBS (pH 7.4) containing 4.0 mM $K_3Fe(CN)_6$ (**a**) and 1.0 mM $Ru(NH_3)_6Cl_3$ (**b**) on bare GCE (*a*), ERGO/GCE (*b*), PPy/ERGO/GCE (*c*) and OPPy/ERGO/GCE (*d*) at scan rate of 50 mV s^{-1}

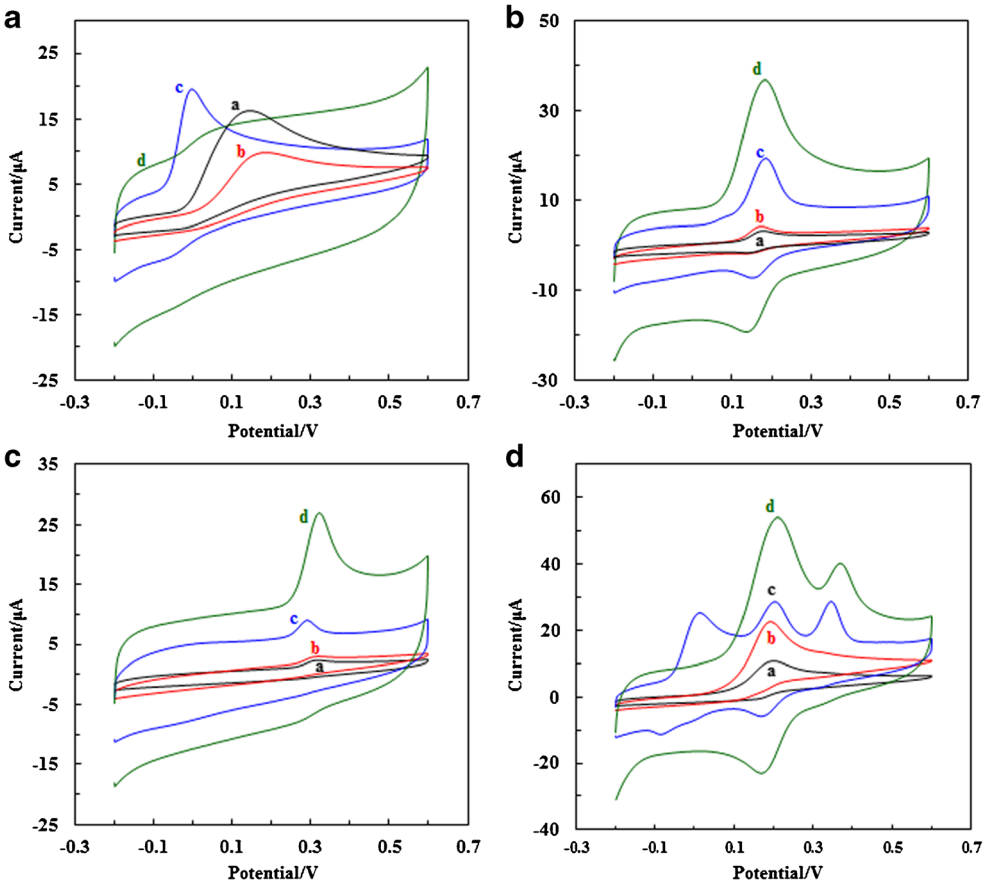

Fig. 4 Cyclic voltammograms of 1.0 mM AA (**a**), 0.1 mM DA (**b**), 0.1 mM UA (**c**) and a mixture of 1.0 mM AA, 0.1 mM DA and 0.1 mM UA (**d**) on bare GCE (*a*), OPPy/GCE (*b*), ERGO/GCE (*c*) and OPPy/ERGO/GCE (*d*) in 10 mM PBS (pH 7.4) at scan rate of 50 mV s^{-1}

selectivity of overoxidized polypyrrole, as well as the synergistic effects between graphene and OPPy.

Furthermore, comparison of the electrochemical behaviors of the single component of AA, DA and UA, and the mixture of AA, DA and UA on PPy/GCE and OPPy/GCE, PPy/ERGO/GCE and OPPy/ERGO/GCE (as shown in Fig. S1), demonstrates again that the overoxidation process for the PPy/ERGO hybrid composite has the crucial significance on its electrocatalytic activity, cation selectivity, as well as the synergistic effects. As expected, the electrochemical performances and applications of OPPy/ERGO/GCE in selective and sensitive determination of DA are worthy of further exploration.

Electrochemical beheviors of OPPy/ERGO/GCE towards DA

The electrochemical behaviors of 0.1 mM DA in 10 mM PBS with pH values of 4.4, 5.4, 6.4, 7.4 and 8.4 at OPPy/ERGO/GCE were investigated by cyclic voltammetry, respectively. From Fig. 5a, it can be seen that the redox peak currents dramatically decreased when the pH value exceeds 7.0. This is due to the cationic selectivity of the OPPy film and the positive charge of DA under acidic conditions. However, considering that the physiological pH value is 7.4, pH 7.4 was chosen as the pH value of the supporting electrolyte in the following electrochemical determination of DA. Additionally, Fig. 5b shows that both the oxidation peak potentials and the reduction peak potentials of DA have a good linear relationship with pH values and the linear regression equations are $E_{pa} = -0.046\ pH + 0.53$ (R = 0.9932) and $E_{pc} = -0.050\ pH + 0.53$ (R = 0.9926), respectively. The redox peak potentials shifted with the increasing of pH values, indicating that the redox reaction of DA at OPPy/ERGO/GCE is accompanied by proton transfer. And the slope of −46 mV pH^{-1} and 50 mV pH^{-1} are close to the theoretical value, which indicates that equal number of electrons and protons transfer process.

The kinetics of electrode reaction was investigated by exploring the redox peak currents of DA dependence on the scan rates. Figure 5c displays the cyclic voltammograms of OPPy/ERGO/GCE in 10 mM PBS (pH 7.4) containing 0.1 mM DA with the scan rate ranging from 20 mV s^{-1} to 600 mV s^{-1}. From Fig. 5d, it can be seen that both the absolute values of oxidation peak currents (line a) and reduction peak currents (line b) linearly increase with the scan rates. The linear regression equations are expressed as follows: I_{pa} (μA) = 0.33 v (mV s^{-1}) + 29 (R = 0.9902), I_{pc} (μA) = −0.17 v (mV s^{-1}) - 6.2 (R = 0.9981). And both the absolute values of the oxidation and reduction peak potentials increase with logarithmic of the scan rates (lines c and d). The change is small at low scan rates (below 200 mV s^{-1}) but

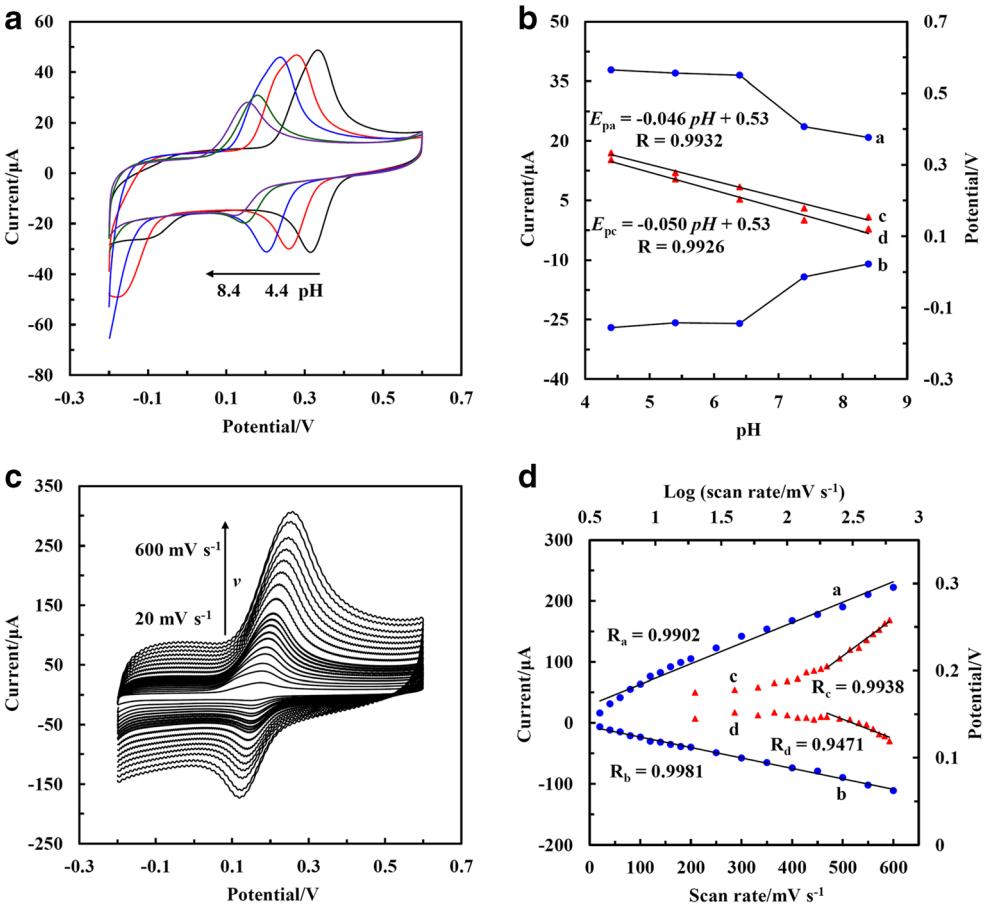

Fig. 5 **a** Cyclic voltammogram of 0.1 mM DA in 10 mM PBS with pH values of 4.4, 5.4, 6.4, 7.4, 8.4 on OPPy/ERGO/GCE at scan rate of 50 mV s^{-1} and **b** the effect of pH on the redox peak currents and potentials. **c** Cyclic voltammograms of 0.1 mM DA in 10 mM PBS (pH 7.4) on OPPy/ERGO/GCE at different scan rates of 20, 40, 60, 80, 100, 120, 140, 160, 180, 200, 250, 300, 350, 400, 450, 500, 550, 600 mV s^{-1} and **d** the plots of redox peak currents and potentials versus scan rate or the logarithm of scan rate. Lines a and b are the plots of peak currents, and lines c and d are the plots of peak potentials

increases linearly at high scan rates (above 200 mV s^{-1}). These results indicate that the electrochemical process of DA at the OPPy/ERGO/GCE is a surface-confined process with relatively slow electron transfer [28].

Electrochemical determination of dopamine (DA)

Figure 6a and b shows differential pulse voltammograms at OPPy/ERGO/GCE for the different concentrations of DA in 10 mM PBS (pH 7.4) with the absence (Fig. 6a) and the presence (Fig. 6b) of 1.0 mM AA and 0.1 mM UA. From the inset of Fig. 6a, it can be seen that the oxidation peak currents I_{pa} linearly increases with increasing of the DA concentrations from 2.0 to 160 μM, and linear regression equation is calibrated as I_{pa} (μA) = 0.33 C (μM) + 0.94 with the correlation coefficient R was 0.9988 and the detection limit of 0.5 μM is calculated based on S/N of 3. It should be noted that there is a shoulder oxidation peak appears at about +0.050 V when the DA concentration is over 80 μM. This is probably ascribed to the oxidation process of the adsorbed DA on the electrode surface, which confirmed by cyclic voltammetry in the different concentrations of DA (as shown in Fig. S2). From Fig. 6b, an extremely weak oxidation peak of AA can be seen at the lower concentrations of DA, and the oxidation peaks of AA, DA and UA can be distinguished definitely. The inset of Fig. 6b shows that the voltammetric response currents I_{pa} as well as in the absence of AA and UA solution, linearly increases with the concentrations of DA in the range from 2.0 to 160 μM with the detection limit of 0.5 μM (S/N = 3). The linear regression equation is calibrated as I_{pa} (μA) = 0.36 C (μM) + 0.04 with the correlation coefficient R of 0.9982.

Compared with voltammetry, chronoamperometry has higher sensitivity and is more suitable for real-time online analysis, so it is also used for the detection of dopamine. The operated oxidation potential is optimized to 0.22 V (as shown in Fig. S3). Figure 6c shows amperometric response of OPPy/ERGO/GCE at +0.22 V to the consecutive addition of DA in 10 mM PBS (pH 7.4). The ladder-shaped oxidation current increases linearly with the concentration of DA in the range of 0.4 to 517 μM, and the linear equation is calibrated as I (μA) = −0.043 C (μM) + 1.1 with the correlation coefficient R of 0.9929 and the detection limit of 0.2 μM (S/N = 3). Both the linear range and limit of detection obtained by DPV and amperometry at the OPPy/ERGO/GCE for the determination of DA are comparing favourably with other studies are summarized in Table 1. As shown in Fig. 6d, the interference effect was evaluated by chronoamperometry. It can be seen that the same concentration of AA and UA, 50-fold of

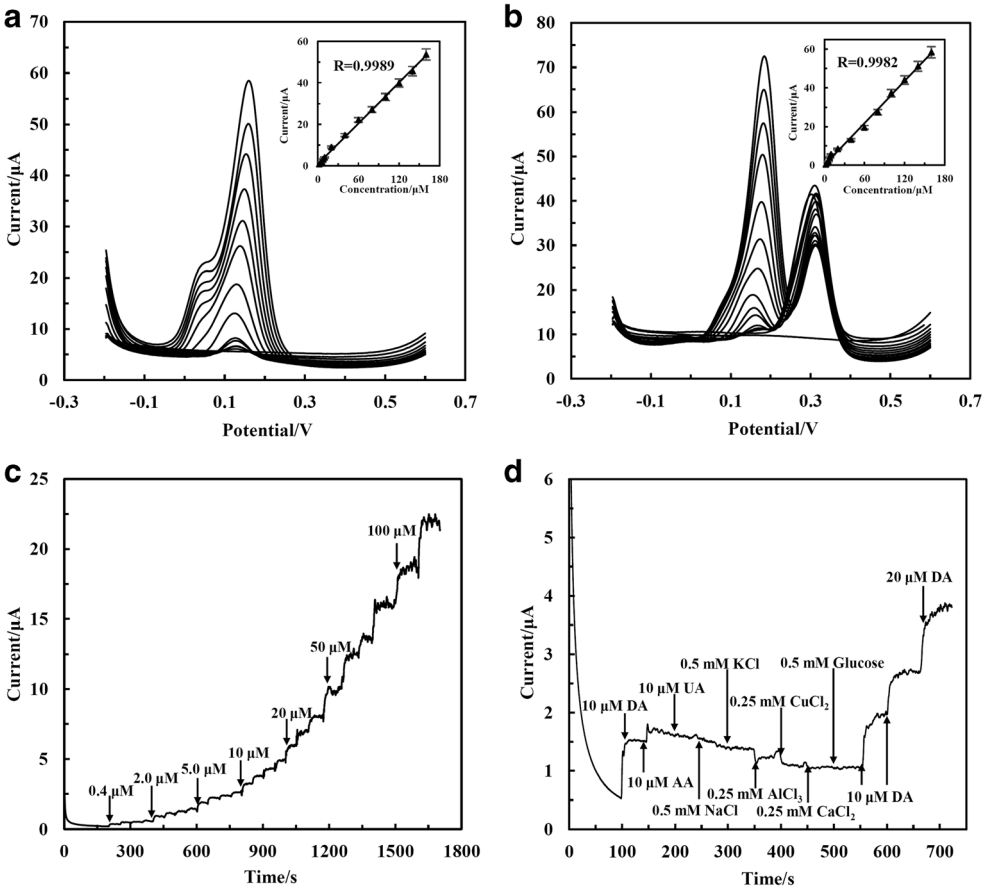

Fig. 6 Differential pulse voltammograms on OPPy/ERGO/GCE in 10 mM PBS (pH 7.4) containing DA concentrations of 0, 2.0, 4.0, 6.0, 8.0, 10, 20, 40, 80, 100, 120, 140 and 160 μM in the absence (**a**) and the presence (**b**) of 1.0 mM AA and 0.1 mM UA at scan rate of 50 mV s^{-1}. **c** Amperometric responses of OPPy/ERGO/GCE at +0.22 V upon successive addition of DA into stirring 10 mM PBS (pH 7.4). **d** Amperometric responses of OPPy/ERGO/GCE upon the addition of 10 μM DA, 10 μM AA, 10 μM UA, 0.5 mM NaCl, 0.5 mM KCl, 0.25 mM $AlCl_3$, 0.25 mM $CuCl_2$, 0.25 mM $CaCl_2$, 0.5 mM glucose and 20 μM DA, respectively. The insets show linear calibration plots of currents versus DA concentrations

Table 1 Comparison of the proposed OPPy/ERGO hybrids modified GCE with other electroanalytical methods for the determination of DA

Modified materials	Linear range (μM)	Detection limit (μM)	Sensitivity (μA $μM^{-1}$)	Method	Ref.
Graphene	4.0–100	2.6	0.066	DPV	[29]
Graphene oxide	1.0–15	0.27	0.55	DPV	[30]
Graphene-PEDOT [a]	1.0–150	0.33	0.22	DPV	[31]
Graphene-AuNPs	5.0–1000	1.9	0.036	DPV	[32]
α-Fe_2O_3@ERGO	0.25–100	0.024	0.22	LSV [b]	[33]
ERGO-poly-L-lysine	2.0–60	0.10	2.7	DPV	[4]
ZnNi NPs@MWCNTs	250–1700	0.066	/ [c]	DPV	[5]
RGO-CdSe QD	4.9–74	0.11	0.16	DPV	[6]
AgNC@PDA-NS [d]	2.5–130	0.25	0.54	DPV	[7]
PTCA-RGO-MWCNTs-AuNPs [e]	1.0–125	0.07	0.12	Amperometry	[34]
GO/AuNPs/pDAN-EDTA [f]	0.01–1	0.005	0.010	Amperometry	[35]
OPPy/ERGO	2.0–160 0.4–517	0.5	0.33	DPV	This work

[a] PEDOT: poly(3,4-ethylenedioxythiophene)

[b] LSV: linear sweep voltammetry

[c] Did not report in their work

[d] AgNC: silver nanocube, PDA-NS: polydopamine nanosphere

[e] PTCA: 3,4,9,10-perylene tetracarboxylic acid, MWCNTs: multi-walled carbon nanotubes

[f] pDAN: polydiaminonaphthalene, EDTA: Ethylenediaminetetraacetic acid

NaCl and KCl, 25-fold of $AlCl_3$, $CuCl_2$ and $CaCl_2$, and 50-fold of glucose do not interfere with the oxidation signal of DA (oxidation current change <±5%). Additionally, the OPPy/ERGO modified electrode is stable for at least one month, which the oxidation current decreased smaller than 5% for DA. Furthermore, the modified electrode was applied to determination of DA in human urine sample, which was diluted 500 times with 10 mM PBS (pH = 7.4) before the measurement. When known amounts of DA were added to the real samples, quantitative recovery from 96.5% to 99.0% was satisfied (Table S1). These attractive features of the OPPy/ERGO/GCE suggest a promising application for the determination of DA in physiological and pathological conditions.

Conclusion

A novel graphene-based hybrid material OPPy/ERGO was prepared and applied in selective and sensitive determination of DA in the presence of AA and UA under physiological pH conditions. It was demonstrated that the OPPy/ERGO/GCE shows excellent electrocatalytic activities towards the oxidation of DA and UA and inhibiting effect for the oxidation of AA, which is mainly ascribed to the electrocatalytic activity, cation selectivity, as well as the synergistic effects between ERGO and OPPy. It should be noted that the overoxidation process for the PPy/ERGO hybrid nanocomposite has the crucial significance on the electrochemically analytical properties. In addition, a higher concentrations of AA (100-fold) still has a certain amperometric oxidation response, which will interfere with the amperometric detection of a lower concentrations of DA. The work demonstrated that attractive features of OPPy/ERGO is expected to provide promising applications in the determination of DA in physiological and pathological conditions.

Acknowledgements This work was supported by the National Natural Science Foundation of China (No.21305106) and Shaanxi Province Natural Science Foundation of China (No.2019JM-469).

Compliance with ethical standards The author(s) declare that they have no competing interests.

References

1. Janezic S, Threlfell S, Dodson PD, Dowie MJ, Taylor TN, Potgieter D, Parkkinen L, Senior SL, Anwar S, Ryan B, Deltheil T, Kosillo P, Cioroch M, Wagner K, Ansorge O, Bannerman DM, Bolam JP, Magill PJ, Cragg SJ, Wade-Martins R (2013) Deficits in dopaminergic transmission precede neuron loss and dysfunction in a new Parkinson model. Proc Natl Acad Sci U S A 110:E4016–E4025
2. Bucher ES, Wightman RM (2015) Electrochemical analysis of neurotransmitters. Annu Rev Anal Chem 8:239–261
3. Xiao T, Wu F, Hao J, Zhang M, Yu P, Mao L (2017) In vivo analysis with electrochemical sensors and biosensors. Anal Chem 89:300–313
4. Zhang D, Li L, Ma W, Chen X, Zhang Y (2017) Electrodeposited reduced graphene oxide incorporating polymerization of l-lysine on electrode surface and its application in simultaneous electrochemical determination of ascorbic acid, dopamine and uric acid. Mat Sci Eng C-Mater 70:241–249
5. Savk A, Özdil B, Demirkan B, Nas MS, Calimli MH, Alma MH, Inamuddin AAM, Şen F (2019) Multiwalled carbon nanotube-based nanosensor for ultrasensitive detection of uric acid, dopamine and ascorbic acid. Mat Sci Eng C-Mater 99:284–254
6. Tavakolian E, Tashkhourian J (2018) Sonication-assisted preparation of a nanocomposite consisting of reduced graphene oxide and CdSe quantum dots, and its application to simultaneous voltammetric determination of ascorbic acid, dopamine and uric acid. Microchim Acta 185:456–463
7. Li Y, Jiang Y, Song Y, Li Y, Li S (2018) Simultaneous determination of dopamine and uric acid in the presence of ascorbic acid using a gold electrode modified with carboxylated graphene and silver nanocube functionalized polydopamine nanospheres. Microchim Acta 185:382–391
8. Kepinska D, Blanchard GJ, Krysinski P, Stolarski J, Kijewska K, Mazur M (2011) Pyrene-loaded polypyrrole microvessels. Langmuir 27:12720–12729
9. Schuhmann W (1995) Electron-transfer pathways in amperometric biosensors. Ferrocenemodified enzymes entrapped in conducting-polymer layers. Biosens Bioelectron 10:181–193
10. Kim J-H, Sharma AK, Lee Y-S (2006) Synthesis of polypyrrole and carbon nano-fiber composite for the electrode of electrochemical capacitors. Mater Lett 60:1697–1701
11. Diaz AF, Kanazaw KK (1979) Electrochemical polymerization of pyrrole. Chem Commun 14:635–636
12. Beck F, Braun P, Oberst M (1987) Organic electrochemistry in the solid state-overoxidation of polypyrrole. Ber Bunsenges Phys Chem 91:967–974
13. Witkowski A, Freund MS, Brajter-Toth A (1991) Effect of electrode substrate on the morphology and selectivity of overoxidized polypyrrole films. Anal Chem 63:622–626
14. Witkowski A, Brajter-Toth A (1992) Overoxidized polypyrrole films: a model for the design of permselective electrodes. Anal Chem 64:635–641
15. Freund M, Eodalbhai L, Brajter-Toth A (1991) Anion excluding polypyrrole films. Talanta 38:95–99
16. Pihel K, Walker QD, Wightman RM (1996) Overoxidized polypyrrole-coated carbon fiber microelectrodes for dopamine measurements with fast-scan cyclic voltammetry. Anal Chem 68: 2084–2089
17. Chen A, Chatterjee S (2013) Nanomaterials based electrochemical sensors for biomedical applications. Chem Soc Rev 42:5425–5438
18. Novoselov KS, Geim AK, Morozov SV, Jiang D, Zhang Y, Dubonos SV, Grigorieva IV, Firsov AA (2004) Electric field effect in atomically thin carbon films. Science 306:666–669
19. Ambrosi A, Chua CK, Bonanni A, Pumera M (2014) Electrochemistry of graphene and related materials. Chem Rev 114:7150–7188
20. Su Z, Xu X, Cheng Y, Tan Y, Xiao L, Tang D, Jiang H, Qin X, Wang H (2019) Chemical pre-reduction and electro-reduction guided preparation of a porous graphene bionanocomposite for indole-3-acetic acid detection. Nanoscale 11:962–967
21. Chen L, Tang Y, Wang K, Liu C, Luo S (2011) Direct electrodeposition of reduced graphene oxide on glassy carbon electrode and its electrochemical application. Electrochem Commun 13:133–137

22. Zhang D, Ouyang X, Ma W, Li L, Zhang Y (2016) Voltammetric determination of folic acid using adsorption of methylene blue onto electrodeposited of reduced graphene oxide film modified glassy carbon electrode. Electroanalysis 28:312–319
23. Wang J, Jiang M (2000) Toward genolelectronics: nucleic acid doped conducting polymers. Langmuir 16:2269–2274
24. Tiwari I, Gupta M, Pandey CM, Mishra V (2015) Gold nanoparticle decorated graphene sheet-polypyrrole based nanocomposite: its synthesis, characterization and genosensing application. Dalton Trans 44:15557–15566
25. Daniel Arulraj A, Arunkumar A, Vijayan M, Balaji Viswanath K, Vasantha VS (2016) A simple route to develop highly porous nano polypyrrole/reduced graphene oxide composite film for selective determination of dopamine. Electrochim Acta 206:77–85
26. Liu H, Gao J, Xue M, Zhu N, Zhang M, Cao T (2009) Processing of graphene for electrochemical application: noncovalently functionalize graphene sheets with water-soluble electroactive methylene green. Langmuir 25:12006–12010
27. Zhu C, Zhai J, Wen D, Dong S (2012) Graphene oxide/polypyrrole nanocomposites: one-step electrochemical doping, coating and synergistic effect for energy storage. J Mater Chem 22:6300–6306
28. Zhang D, Fu L, Liao L, Dai B, Zou R, Zhang C (2012) Electrochemically functional graphene nanostructure and layer-by-layer nanocomposite incorporating adsorption of electroactive methylene blue. Electrochim Acta 75:71–79
29. Kim YR, Bong S, Kang YJ, Yang Y, Mahajan RK, Kim JS, Kim H (2010) Electrochemical detection of dopamine in the presence of ascorbic acid using graphene modified electrodes. Biosens Bioelectron 25:2366–2369
30. Gao F, Cai X, Wang X, Gao C, Liu S, Gao F, Wang Q (2013) Highly sensitive and selective detection of dopamine in the presence of ascorbic acid at graphene oxide modified electrode. Sensors Actuators B 186:380–387
31. Xu G, Jarjes ZA, Desprez V, Kilmartin PA, Travas-Sejdic J (2018) Sensitive, selective, disposable electrochemical dopamine sensor based on PEDOT-modified laser scribed graphene. Biosens Bioelectron 107:184–191
32. Li J, Yang J, Yang Z, Li Y, Yu S, Xua Q, Hu X (2012) Graphene-au nanoparticles nanocomposite film for selective electrochemical determination of dopamine determination of dopamine. Anal Methods 4:1725–1728
33. Mathew G, Dey P, Das R, Chowdhury SD, Paul Das M, Veluswamy P, Neppolian B, Das J (2018) Direct electrochemical reduction of hematite decorated graphene oxide (alpha-Fe_2O_3@erGO) nanocomposite for selective detection of Parkinson's disease biomarker. Biosens Bioelectron 115:53–60
34. Zhang C, Ren J, Zhou J, Cui M, Li N, Han B, Chen Q (2018) Facile fabrication of a 3,4,9,10-perylene tetracarboxylic acid functionalized graphene-multiwalled carbon nanotube-gold nanoparticle nanocomposite for highly sensitive and selective electrochemical detection of dopamine. Analyst 143:3075–3084
35. Mir TA, Akhtar MH, Gurudatt NG, Kim JI, Choi CS, Shim YB (2015) An amperometric nanobiosensor for the selective detection of K(+)-induced dopamine released from living cells. Biosens Bioelectron 68:421–428